

A Phenomenological Model for Wind Speed and Shear Stress Profiles in Vegetation Cover Layers

F. A. ALBINI

*U.S. Department of Agriculture Forest Service, Intermountain Forest and Range Experiment Station,
Northern Forest Fire Laboratory Missoula, MT 59801*

(Manuscript received 18 February 1981, in final form 2 August 1981)

ABSTRACT

A phenomenological model for the mean wind speed and Reynolds shear stress profiles with height in a vegetation cover layer is derived from forms suggested by truncation of the equations of turbulent fluid motion at second order in fluctuating velocity products. The initial formulation is unique in that the force per unit volume resisting fluid motion is treated as a body force having a height-dependent character. The body force is assumed to be proportional to the instantaneous speed squared and in the opposite direction from the instantaneous velocity. Viscous forces are ignored as are all pressure forces except for a steady vertical pressure gradient. Closure of the equations is effected by a phenomenological assumption linking the static pressure and the square of the mean wind speed. The mean wind speed profile predicted by the model is an exponential in the cumulative drag area per unit planform area as a function of height, which is a simple exponential in height for cover with uniform plant area density. Comparisons of predicted profiles of wind speed and Reynolds shear stress with measurements show the model to be relatively robust.

1. Introduction

The motion of air over and within vegetation cover has been a subject of research for many years. Agronomists and microclimatologists seek an understanding of the environment within vegetation and the interaction of it with the atmosphere at large (Monteith, 1975). Meteorologists concerned with events on larger scales need to deal with vegetation cover as it influences boundary conditions of the transport equations with which they describe the atmosphere (Plate, 1971; Oke, 1978; Maitani, 1979a). In addition, prediction of the behavior and effects of a wildland fire requires knowledge of the influence of vegetation cover on the wind field that interacts with the fire (Albini and Baughman, 1979; Baughman and Albini, 1980).

The quest for a simple yet robust phenomenological model for the profile of wind speed within vegetation cover has engaged many investigators (Inoue, 1963; Cionco, 1965, 1972a, 1978; Cowan, 1968; Landsberg and James, 1971; Thom, 1971). Other studies, analytical and experimental, have focused on the wind velocity fluctuations that provide the mechanisms of turbulent shear stress and energy transport (Allen, 1968; McBean, 1968; Meroney, 1968; Cionco, 1972b; Silversides, 1974; Shaw *et al.*, 1974; Hicks and Sheih, 1977; Maitani, 1977a,b, 1978, 1979a). Analytical efforts that sacrifice simplicity for generality and greater understand-

ing of the processes at work in the interactions between vegetation and the atmosphere have become increasingly complex and detailed as digital computing capability has grown (Bergen, 1975; Kondo and Akashi, 1976; Wilson and Shaw, 1977; Shaw, 1977). Recent models have sought to include explicitly the motion of the vegetation (Finnigan and Mulhearn, 1978a,b; Finnigan, 1979b). Experiments in wind tunnels have played an important part in model development by providing repeatable, controlled conditions under which specific relationships have been investigated (Plate and Quraishi, 1965; Meroney, 1968; Hsi and Nath, 1970; Thom 1971; Seginer *et al.*, 1976; Finnigan and Mulhearn, 1978b; Finnigan, 1979a).

The simplest description of the flow field in vegetation cover consists of a single component of the momentum equation in which the drag force per unit volume afforded by the plant components is balanced by the vertical gradient of horizontal turbulent shear stress. Phenomenological models based on Prandtl's mixing length theory (Schlichting, 1968) are often used to express the shear stress in terms of the vertical gradient of the mean horizontal wind speed. Specification of the characteristic "mixing length" then closes the set of equations, permitting derivation of expressions for the wind speed profile. Inoue (1963) and Cionco (1965, 1972a) assumed a constant value for the mixing length for idealized crop canopies, while Kondo and Akashi

(1976) derive it from von Kármán's ratio (Schlichting 1968) subject to some constraints. Cowan (1968) took the square of the mixing length to be proportional to the ratio of the mean wind speed to its gradient, resulting in a shear stress proportional to the gradient of the square of the mean wind speed. Thom (1971) and Landsberg and James (1971) assumed the shear stress proportional to the gradient of the mean wind speed. This sidesteps the question of a mixing length entirely but can be interpreted as taking the mixing length to be inversely proportional to the square root of the mean velocity gradient.

Higher order closure models have been proposed (Bergen, 1975; Wilson and Shaw, 1977; Shaw, 1977) involving the introduction of additional equations and parameters. Solutions using these models are achievable only with the aid of digital computers.

While all the models mentioned provide predictions that agree reasonably well with measured velocity and shear stress profiles, the diversity of forms for the shear stress is disconcerting. And while all involve the introduction of a length scale in one form or another, none make extensive use of an intrinsic length scale of the vegetation cover in deriving the shear stress. This scale is the inverse of the drag area per unit volume of the vegetation cover layer viewed as a continuum.

The model presented in this paper is suggested by a second-order closure of the equations of motion made possible by treating the vegetation layer as a continuum imposing a square law body force on the fluid. This treatment yields an equation for the turbulent shear stress as a function of the mean horizontal wind speed and the vegetation's drag area per unit volume. An explicit shear stress model of this type is ultimately needed for the development of a description of the processes involved in the combustion of standing vegetation in a wildland fire. The resulting expression for the wind speed profile can be approximated accurately by the exponential of the integral over height of the drag area density of the plant parts. Calculated wind speed and shear stress profiles are similar to the predictions of other phenomenological models and can be fitted well to published experimental data. The simplicity and generality of the model are appealing and the continuum treatment invites test and extension.

2. Model development

For the present purposes, the atmosphere is assumed to be neutrally stable, incompressible and inviscid. No horizontal static pressure gradient is considered and Coriolis acceleration is disregarded. The coordinate system used is Cartesian, with x in the direction of the mean horizontal wind speed, y the lateral orthogonal, and z vertical upward from

the surface of the earth. The velocity components in these three directions are u , v and w , respectively. The pressure field, compensated by the hydrostatic vertical distribution and divided by the (constant) air density, is represented by p . An overbar on a velocity component represents a (long-term) temporal mean, a prime denotes a temporal deviation from the mean, and an unmarked symbol the sum of the two.

Neglecting viscous stresses limits the applicability of the equations to that region of the flow field in which the Reynolds stresses predominate. This is a sound approximation for most of the vegetation cover layer; the viscous sublayer will be ignored and the turbulent fluid description extended to the surface. But explicit dismissal of viscosity leads inevitably to equations that will not degenerate to a shear layer description in the vegetation-free limit, so an implicit restriction on cover-layer, drag-area density resides in this approximation as well. It is easy to show that such a limitation also substantiates ignoring Coriolis acceleration.

Treating air as an incompressible fluid introduces no significant error and restriction to neutral stability avoids the complication of buoyancy influences.

Inclusion of a horizontal static pressure gradient adds a driving force to the equations of motion that is not necessarily aligned with the direction of air flow over the vegetation canopy, resulting in a height-dependent wind direction that can vary significantly for tall crops or forests (Shinn, 1971). For the present, attention is restricted to flows free of horizontal static pressure gradients simply to make the analysis more tractable and transparent. Pressure gradient terms are included formally in the development that follows, but ultimately only a vertical steady pressure gradient is retained.

Under the stated assumptions, the equations of motion for the wind in the vegetation layer, idealized as a two-dimensional, horizontally homogeneous continuum of height H , can be written as

$$\frac{\partial u}{\partial t} + \frac{\partial u^2}{\partial x} + \frac{\partial uv}{\partial y} + \frac{\partial uw}{\partial z} = -Jus - \frac{\partial p}{\partial x}, \quad (1)$$

$$\frac{\partial v}{\partial t} + \frac{\partial uv}{\partial x} + \frac{\partial v^2}{\partial y} + \frac{\partial vw}{\partial z} = -Jvs - \frac{\partial p}{\partial y}, \quad (2)$$

$$\frac{\partial w}{\partial t} + \frac{\partial uw}{\partial x} + \frac{\partial vw}{\partial y} + \frac{\partial w^2}{\partial z} = -Jws - \frac{\partial p}{\partial z}, \quad (3)$$

$$\begin{aligned} \frac{\partial s^2}{\partial t} + \frac{\partial us^2}{\partial x} + \frac{\partial vs^2}{\partial y} + \frac{\partial ws^2}{\partial z} \\ = -2Js^3 - 2\left(u \frac{\partial}{\partial x} + v \frac{\partial}{\partial y} + w \frac{\partial}{\partial z}\right)p, \quad (4) \end{aligned}$$

where t is time, s the local speed $(u^2 + v^2 + w^2)^{1/2}$, and J the local drag area per unit volume. The drag

force here is assumed to be proportional to the square of the local speed and to be in the opposite direction from the local velocity. The drag coefficient of the plant parts being independent of the local speed implies that the local Reynolds number is high (Schlichting, 1968), which is consistent with ignoring viscous stresses. The first three equations express the momentum balance in the three principal directions and (4) the conservation of energy.

To establish additional relationships at the second order, we multiply (1) by w , (3) by u , and sum, making use of the continuity equation

$$\frac{\partial u}{\partial x} + \frac{\partial v}{\partial y} + \frac{\partial w}{\partial z} = 0. \tag{5}$$

Performing the corresponding multiplications and sums on (1) and (2) and on (2) and (3) gives the needed additional set of relationships:

$$\begin{aligned} \frac{\partial uw}{\partial t} + \frac{\partial u^2 w}{\partial x} + \frac{\partial uvw}{\partial y} + \frac{\partial uw^2}{\partial z} \\ = -2Juws - w \frac{\partial p}{\partial x} - u \frac{\partial p}{\partial z}, \end{aligned} \tag{6}$$

$$\begin{aligned} \frac{\partial uv}{\partial t} + \frac{\partial u^2 v}{\partial x} + \frac{\partial uv^2}{\partial y} + \frac{\partial uvw}{\partial z} \\ = -2Juv s - v \frac{\partial p}{\partial x} - u \frac{\partial p}{\partial y}, \end{aligned} \tag{7}$$

$$\begin{aligned} \frac{\partial vw}{\partial t} + \frac{\partial uvw}{\partial x} + \frac{\partial v^2 w}{\partial y} + \frac{\partial vw^2}{\partial z} \\ = -2Jvws - w \frac{\partial p}{\partial y} - v \frac{\partial p}{\partial z}. \end{aligned} \tag{8}$$

In each of the equations above, we express each variable in terms of its temporal mean and fluctuating parts and then expand all algebraic expressions to second order in fluctuating velocity products and average the resulting equations over time. Example expansions and time averages of the terms involving the instantaneous local speed s are listed below:

$$s_0^2 = \bar{u}^2 + \bar{v}^2 + \bar{w}^2, \tag{9}$$

$$\begin{aligned} \bar{s} = s_0 + (\overline{u'u'} + \overline{v'v'} + \overline{w'w'})/2s_0 \\ - (\bar{u}^2 \overline{u'u'} + \bar{v}^2 \overline{v'v'} + \bar{w}^2 \overline{w'w'})/2s_0^3 \\ - (\bar{u}\bar{v} \overline{u'v'} + \bar{u}\bar{w} \overline{u'w'} + \bar{v}\bar{w} \overline{v'w'})/s_0^3, \end{aligned} \tag{10}$$

$$\bar{s}^2 = s_0^2 + \overline{u'u'} + \overline{v'v'} + \overline{w'w'}, \tag{11}$$

$$\begin{aligned} \bar{s}^3 = s_0^2 \bar{s} + s_0(\overline{u'u'} + \overline{v'v'} + \overline{w'w'}) \\ + 2(\bar{u}\overline{u'u's} + \bar{v}\overline{v'v's} + \bar{w}\overline{w'w's}), \end{aligned} \tag{12}$$

$$\overline{u's} = (\bar{u}\overline{u'u'} + \bar{v}\overline{u'v'} + \bar{w}\overline{u'w'})/s_0, \tag{13}$$

$$\overline{u'w's} = \overline{u'w'}s_0. \tag{14}$$

Carrying out the expansions and time averages

indicated gives the equations for the mean fluid velocities and products of fluctuating components of second order. The steady, one-dimensional case under study is described by taking \bar{v} and \bar{w} to be zero, along with derivatives with respect to t , x and y , i.e.,

$$\frac{d}{dz} \overline{u'w'} = -J(\bar{u}\bar{s} + \overline{u's}), \tag{15}$$

$$\frac{d}{dz} \overline{v'w'} = -J(\overline{v's}) = -J\overline{u'v'}, \tag{16}$$

$$\frac{d}{dz} \overline{w'w'} = -J(\overline{w's}) - \frac{d\bar{p}}{dz} = -J\overline{u'w'} - \frac{d\bar{p}}{dz}, \tag{17}$$

$$\frac{d}{dz} \overline{w's^2} = -2J\bar{s}^3 - 2\overline{w' \frac{dp'}{dz}}, \tag{18}$$

$$\begin{aligned} \frac{d}{dz} \overline{uw'w'} = -2J(\overline{uw's} + \overline{u'w's}) \\ - \bar{u} \frac{d\bar{p}}{dz} - \overline{u' \frac{dp'}{dz}}, \end{aligned} \tag{19}$$

$$\frac{d}{dz} \overline{uv'w'} = -2J(\overline{uv's} + \overline{u'v's}), \tag{20}$$

$$0 = -2J\overline{v'w's} - \overline{v' \frac{dp'}{dz}}. \tag{21}$$

These equations are further simplified by using the one-dimensional forms for the quantities involving s and by neglecting the terms involving the gradient of fluctuating pressure. The resulting expressions indicate that $\overline{u'v'}$ and $\overline{v'w'}$ are zero, as they should be, leaving the following set to be solved:

$$\frac{d}{dz} \overline{u'w'} = -J(\bar{u}^2 + \overline{u'u'} + \overline{v'v'}/2 + \overline{w'w'}/2), \tag{22}$$

$$\frac{d}{dz} \overline{w'w'} = -J\overline{u'w'} - \frac{d\bar{p}}{dz}, \tag{23}$$

$$\begin{aligned} \frac{d}{dz} \overline{uw'w'} \\ = -J\bar{u}(\bar{u}^2 + 3[\overline{u'u'} + \overline{v'v'}/2 + \overline{w'w'}/2]), \end{aligned} \tag{24}$$

$$\frac{d}{dz} \overline{uw'w'} = -4J\bar{u}\overline{u'w'} - \bar{u} \frac{d\bar{p}}{dz}. \tag{25}$$

The horizontal momentum balance expressed by (22) and the energy transport/dissipation balance expressed by (24) are physically appealing if unfamiliar in form. Since we treat the vegetation layer as a continuum, introducing the drag per unit volume as a dominant fluid body force term is a departure from most previous canopy flow treatments (Cionco, 1965; Bergen, 1975; Shaw, 1977; Wilson and Shaw, 1977). Identical grouping of fluctuating components

in (22) and (24) is intuitively appropriate and simplifies the analysis.

The vertical momentum balance of (23) can be used with (25) to relate the Reynolds shear stress to the vertical velocity fluctuation and mean velocity profiles. Since $\overline{u'w'}$ should obviously be the dominant term in the expansion of $\overline{w's}$ and $\overline{u'w's}$ should be well represented by $(\overline{u'w'})\bar{u}$, the most significant approximations involved in these expressions are neglect of $\overline{u'(dp'/dz)}$ and the third-order term $\overline{u'w'w'}$ in (25).

Truncation of the velocity product expansions at second order clearly limits the realism of this approach. It must be recognized at this point that an accurate description of the fluctuating velocity fields cannot be achieved from the resulting equation set. What is sought, however, is only a phenomenological description of the mean wind-speed profile and the turbulent shear stress, using forms suggested by the abbreviated equations. Reynolds and Cebeci (1978) have argued that any model obtained by truncation at some statistical order will suffer from the defect that equilibrium constitutive relationships are not to be expected at the order of truncation. While such may be true in the case under study here, it does not preclude the possibility of developing robust phenomenological descriptions. It is not clear to what extent the appearance of the square law drag term as a body force on the fluid modifies the theoretical argument of Reynolds. But it is clear from experimental evidence (Allen, 1968; Seginer *et al.*, 1976; Shaw, 1977; Wilson and Shaw, 1977; Maitani 1977a, 1978, 1979a) that higher order velocity fluctuation terms are of a magnitude comparable to the steady terms and so cannot be dismissed if one hopes to describe the turbulence fields accurately.

The products of fluctuating velocity components with fluctuating pressure gradients will exhibit time averages to the extent that the two factors share a frequency range and maintain some degree of phase consistency over it. Since pressure perturbations propagate as acoustical disturbances, the gradient of any particular frequency component is of the order of magnitude of the fluctuation amplitude divided by the wavelength of sound at that frequency. Taking the dynamic pressure as a measure of the fluctuating pressure amplitude (Finnigan, 1979b; Townsend, 1980), the pressure gradient term can be estimated as s^2/λ_0 , where λ_0 is the wavelength of sound at a frequency typical of the fluctuations of the velocity field. In turn, the power spectrum of velocity fluctuations in and above vegetation cover usually has a low-pass filter appearance in that the spectral density is nearly constant below some frequency and declines above that as the inverse 5/3 power of the frequency as is characteristic of the inertial subrange (Allen, 1968; McBean, 1968;

Silversides, 1974; Maitani, 1977b, 1979b; Finnigan, 1979a; Holbo *et al.*, 1980). By this argument the pressure fluctuation terms in the equations above are of the order of magnitude of $1/J\lambda_0$ compared to the body force terms. Since the characteristic frequencies obtained by the investigators just cited are in the range of 0.1 to 1.0 Hz, the pressure fluctuation terms should be negligible so long as the drag area density of the vegetation cover is significantly greater than about 0.01 m^{-1} .

This argument is advanced as heuristic justification for disregarding the fluctuating pressure gradient terms in the energy and cross-product equations. In view of the severity of the approximation implicit in truncation at second order, ignoring these troublesome terms should not be the source of significant added distortion.

A very significant observation to be made about the set of equations above is that the cumulative drag area per unit planform area below physical height z ,

$$\zeta = \int_0^z J dz, \quad (26)$$

is the natural variable of this formulation. This observation rests on only two of the assumptions of this analysis: (i) the vegetation cover layer can be treated as a horizontally homogeneous continuum; and (ii) viscous stresses can be neglected. The other approximations made in the simplification of the equations do not alter this observation.

Performing some obvious manipulations, the equations above can be expressed as

$$\frac{d}{d\zeta} \overline{u'w'} = -\bar{u}^2 + \frac{\overline{u'w'}}{2\bar{u}} \frac{d\bar{u}}{d\zeta}, \quad (27)$$

$$\frac{d}{d\zeta} \overline{w'w'} = -\overline{u'w'} - \frac{d\bar{p}}{d\zeta}, \quad (28)$$

$$\overline{w'w'} \frac{d\bar{u}}{d\zeta} = -3\bar{u}\overline{u'w'}, \quad (29)$$

$$\overline{u'w'} \frac{d\bar{u}}{d\zeta} = -\bar{u}(2\overline{u'u'} + \overline{v'v'} + \overline{w'w'}). \quad (30)$$

Note that if the static pressure gradient in (28) were ignored, the first three equations would be fortuitously closed. The author has explored the model that results from such an assumption. The shear stress and mean wind speed profiles that are predicted appear quite reasonable, but the behavior of the fluctuating velocity component group $\overline{u'u'} + \overline{v'v'}/2$ is physically unrealistic and the model must be considered self-contradictory. Retention of the static pressure gradient adds a further unknown requiring an assumption for closure, but the added degree of freedom permits a model that is at least self-consistent.

From (29) and (30) we have the formal result

$$-\overline{u'w'} = [\overline{w'w'}(2\overline{u'u'} + \overline{v'v'} + \overline{w'w'})/3]^{1/2}, \quad (31)$$

which illustrates the level of realism to be expected in the predicted behavior of the fluctuating velocity components. We shall use this relationship only as a consistency constraint on the behavior of $\overline{w'w'}$, viz., that it vanish at the lower boundary where the shear stress is zero. We shall close the set (27)–(29) by an assumed phenomenological form for the pressure profile. Specifically, we assume that

$$\frac{d\bar{p}}{d\zeta} = -\beta\bar{u} \frac{d\bar{u}}{d\zeta}, \quad (32)$$

where β is a constant (less than unity) to be specified.

Invoking this assumption allows explicit solution for $\overline{w'w'}$ and $\overline{u'w'}$ in terms of \bar{u} (see Appendix):

$$\overline{w'w'} = (3\beta/5)\bar{u}^2 - c\bar{u}^{1/3}, \quad (33)$$

$$-\overline{u'w'} = (B\bar{u} + 2\beta\bar{u}^4/15 - c\bar{u}^{7/3}/2)^{1/2}. \quad (34)$$

The constants B and c are determined by boundary conditions. The boundary conditions used are

At the surface, $z = 0$

$$\zeta = 0; \bar{u} = u_0; \overline{u'w'} = 0, \overline{w'w'} = 0; \bar{p} = p_0. \quad (35)$$

At the top of the cover layer, $z = H$

$$\zeta = \zeta_H; \bar{u} = u_H; -\overline{u'w'} = 1/2 C_f u_H^2; \bar{p} = p_H. \quad (36)$$

Here C_f is a friction coefficient fixed by the boundary layer over the vegetation. Specification of an upper boundary condition on $\overline{w'w'}$ fixes the value of β and hence the pressure distribution. Conversely, specifying a value for the pressure recovery coefficient C_p , where

$$C_p = (p_0 - p_H)/(1/2 u_H^2) = \beta[1 - (u_0/u_H)^2] \quad (37)$$

determines the level of vertical turbulence intensity in this model.

In terms of the boundary variables, the shear stress and vertical turbulence intensity profiles are given in terms of the windspeed profile by

$$-\overline{u'w'} = 1/2 C_f \bar{u}^2 G(u_0/\bar{u})/G(u_0/u_H), \quad (38)$$

$$(\overline{w'w'})^{1/2}/\bar{u}$$

$$= (3C_f/8^{1/2})[1 - (u_0/\bar{u})^{5/3}]^{1/2}/G(u_0/u_H), \quad (39)$$

where the function G is shorthand for

$$G(x) = (1 - 9x^{5/3}/4 + 5x^3/4)^{1/2}. \quad (40)$$

Using (38) in (27) and rearranging gives the equation for the mean wind-speed profile,

$$\frac{d}{d\zeta} \left(\frac{\bar{u}}{u_0} \right) = \left(\frac{10}{3\beta} \right)^{1/2} \left(\frac{\bar{u}}{u_0} \right) \frac{G(u_0/\bar{u})}{1 - (u_0/\bar{u})^{5/3}}. \quad (41)$$

One can readily verify that over the range $0 \leq x \leq 1$

$$(9/10)^{1/2} \leq G(x)/(1 - x^{5/3}) \leq 1, \quad (42)$$

so the wind-speed profile is very well approximated by the exponential

$$\bar{u} = u_0 \exp[(10/3\beta)^{1/2} \zeta]. \quad (43)$$

The exponential form is usually derived under the assumption that the drag area density J is constant (Inoue, 1963; Cionco, 1965) and empirical data descriptions resting on that assumption have proved useful (Cionco 1978). It is interesting that the approach taken here leads to an intuitively appealing extension of that form without invoking the mixing-length hypothesis. Because the mixing-length formulation is so widely used, it is of interest to see how this model relates to it. Using (38) and (43), one can show that the mixing length l implied by the shear stress distribution of this model is a velocity-dependent fraction of $1/J$, falling to zero at the lower boundary and varying as $C_f^{3/2}$:

$$Jl = C_f^{3/2} [9G(u_0/\bar{u})/32G^3(u_0/u_H)]^{1/2}. \quad (44)$$

3. Model predictions of wind speed

Applying the boundary conditions (36) to (43) gives an expression for the ratio u_0/u_H that involves the parameter β . But since β is related to C_f by the upper boundary condition (see Appendix)

$$\beta = 15C_f^2/[8G^2(u_0/u_H)], \quad (45)$$

we have an implicit relationship for u_0/u_H as a function of the ratio ζ_H/C_f :

$$\zeta_H/C_f = \ln[(u_H/u_0)^{3/4}/G(u_0/u_H)]. \quad (46)$$

This equation is graphed in Fig. 1, where we have termed ζ_H the drag area index of the vegetation cover layer.

The functional forms derived here for mean wind speed and shear stress permit these variables to be expressed readily as normalized by their values at the top of the cover layer. For generality, we shall henceforth employ such normalized forms and refer to them as "relative" quantities, e.g., \bar{u}/u_H is called the relative wind speed.

The friction coefficient C_f has been left as a free parameter here, so its value can be assigned from other considerations. For example, if a constant shear layer over the cover exists, then the value of C_f is given in terms of the friction velocity u_* for that layer, i.e.,

$$C_f = 2(u_*/u_H)^2. \quad (47)$$

The logarithmic wind speed profile characteristic of the constant shear layer (Plate, 1971; Grace, 1977) allows one to express u_*/u_H in terms of the zero plane displacement, roughness length and cover height. For the neutrally stable condition this results in a ratio u_*/u_H approximately equal to the von

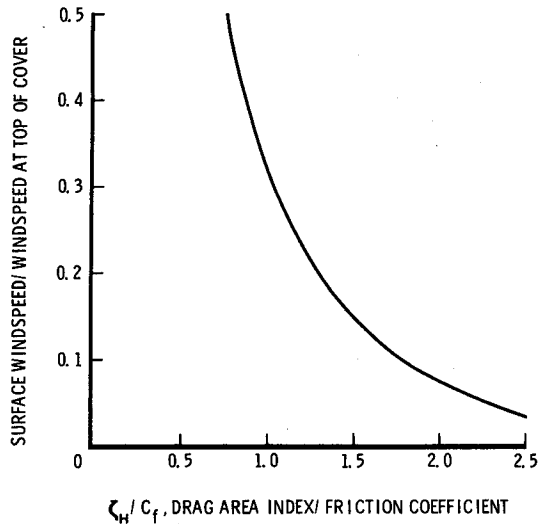


FIG. 1. Ratio of wind speed at the surface to wind speed at the top of the vegetation cover layer as a function of the drag area index divided by the friction coefficient [Eq. (46)].

Kármán constant $K = 0.4$, or a friction coefficient of 0.32 (Baughman and Albin, 1980).

Measurements under various natural conditions (Thom 1971; Jarvis *et al.*, 1976; Leuning and Attwill, 1978; Finnigan, 1979b) have given values of u_*/u_H ranging from 0.19 to 0.50, while wind-tunnel measurements (Meroney, 1968; Hsi and Nath, 1970; Thom, 1971; Seginer *et al.*, 1976) have given friction coefficient values from 0.074 to 0.54.

The drag area index ζ_H should be approximately linearly related to the plant area index or the leaf area index used to characterize vegetation for a variety of purposes (Monteith 1975). It is clearly akin

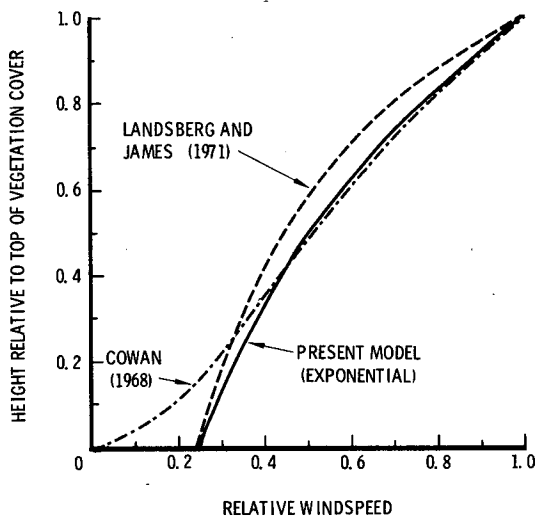


FIG. 2. Comparison of profiles of wind speed in vegetation cover predicted by various phenomenological models for cover with constant drag area density.

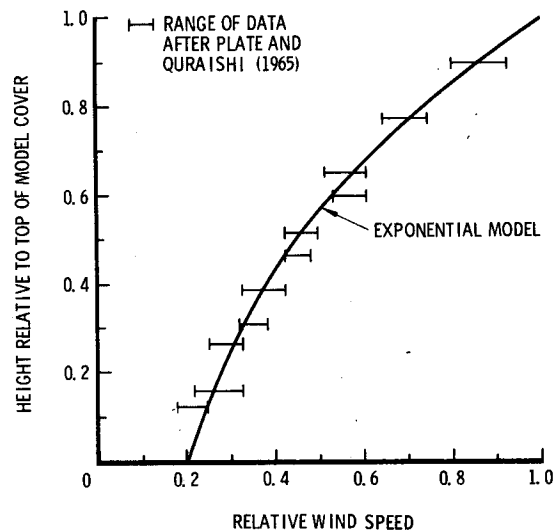


FIG. 3. Experimental data of Plate and Quraishi (1965) with a fitted exponential curve. Any of the models shown in Fig. 2 would describe these data adequately.

to the canopy index of Cionco (1978), but cannot be related uniquely to it until C_f is specified.

The variation of wind speed within the cover layer can be expressed as a function of ζ/ζ_H , which variable should scale with the cumulative distribution of plant area within the layer:

$$\bar{u}/u_H = (u_0/u_H)^{1-\zeta/\zeta_H} \tag{48}$$

This form is convenient for comparison with experimental data when the distribution function for the plant area or leaf area is given. When it can be assumed that the drag area density is about constant, then ζ/ζ_H is simply approximated by z/H . In this case the present model gives wind speed profiles very similar to those predicted by the models of Cowan (1968) and of Landsberg and James (1971) and identical to the "ideal canopy" model of Cionco (1965, 1972a). The model of Cowan (1968) brings the wind speed to zero at the lower surface, but if the relative wind speed given by that model is matched to the exponential prediction midway in the cover layer, the profiles remain very close over most of the layer (Fig. 2). Thus comparison of model predictions with measurements taken in artificial cover layers of high uniformity (Fig. 3) confirm that all these models give a good representation of the wind speed profile in that case, with an appropriate choice of u_0/u_H or by matching prediction to measurement at some point within the cover layer.

In order to compare model predictions to measurements taken in nonuniform cover layers, some means of determining the distribution of drag area density within the cover is needed. Fortunately, some investigators have presented leaf area or plant

area distributions which can be used to convert data on wind speed versus height to wind speed versus cumulative drag area. Fig. 4 (after Shaw, 1977) illustrates this conversion. Using Fig. 4 to convert height to cumulative drag area fraction allows the generation of the curves shown in Fig. 5. Also shown on Fig. 5 are measurements of relative wind speed reported by Shaw (1977). By adjusting the ratio u_0/u_H used in establishing the model profile (illustrated by the two model curves of Fig. 5), a "best" description of the data can be subjectively chosen rather readily.

By using the technique just outlined, model predictions of relative wind speed were made for each anemometer height reported in the studies of maize crops by Cionco (1965) and Shaw *et al.* (1974), and in sunflower by Saugier (1976). The measurements were then plotted against the predictions to produce the scatter diagram shown in Fig. 6. Also shown on that diagram are measurements in artificial uniform cover reported by Thom (1971), Seginer and Mulhearn (1978) and Seginer *et al.* (1976). Finally, data by Inoue (1963) for rice and by Finnigan (1979a) for wheat are shown, under the assumption that these crops exhibit uniform drag area density with height. The agreement between measurements and predictions is at least as good for the nonuniform cover layers as for the others.

The degree of agreement shown in Fig. 6 could no doubt be improved by regressing the experimental data against the predictions and so inferring the "best" value of u_0/u_H for each case. Instead, u_0/u_H was simply chosen subjectively for each data set. The purposes of this comparison are to exhibit the broad applicability of the model and to show that the qualitative features of the experimentally determined wind speed profiles are reproduced.

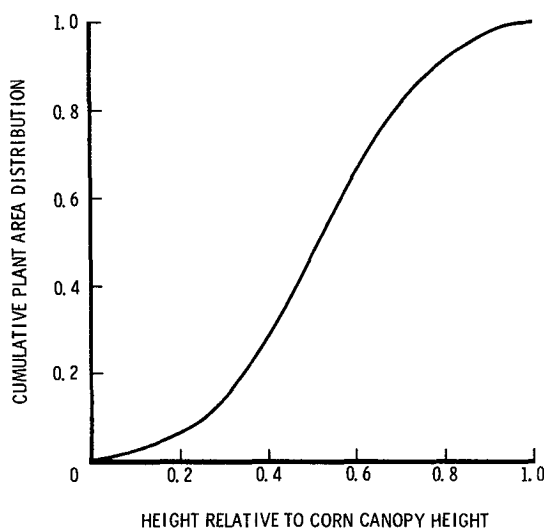


FIG. 4. Cumulative plant area (normalized) versus height for a corn canopy. This curve is after Shaw (1977).

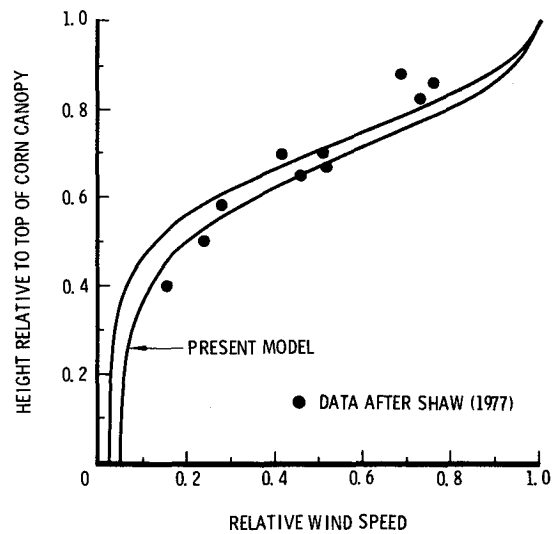


FIG. 5. Using the cumulative plant area distribution of Fig. 4, the present model was used to generate the two curves shown, for comparison with data from Shaw (1977). "Surface" wind speed relative to wind speed at canopy top arbitrarily taken to be 0.025 (left curve) or 0.05 (right curve).

Rauner (1976) used an equation that is the same as (43) to describe data taken in deciduous forest stands, with good results. It should be noted that for forest stands, the drag area density should be maximum near the middle of the tree canopy layer, decreasing to a very small value at the base of the live crown layer and remaining small to the surface, through the subcanopy stem space if such exists. The commonly noted characteristic that the wind speed varies hardly at all from the surface to the

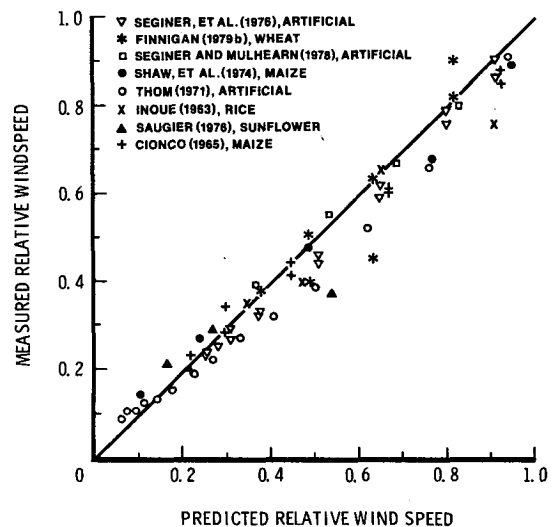


FIG. 6. Following the procedure of Figs. 4 and 5, relative wind speeds were predicted for each anemometer height and cross plotted against the relative wind speeds measured by the various investigators listed on the figure. Rice and wheat crops were assumed to have constant drag area density with height.

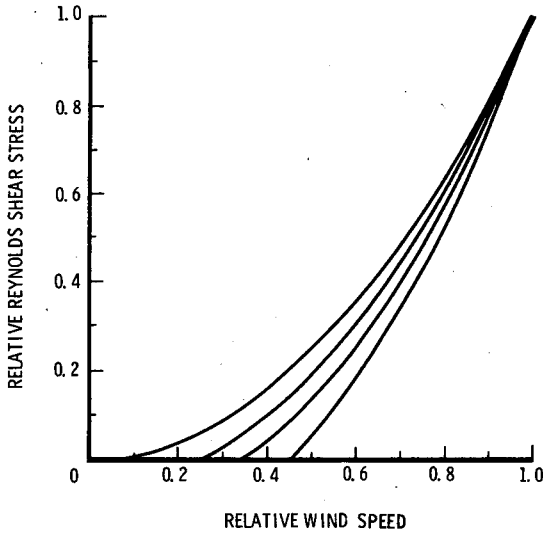


FIG. 7. Reynolds shear stress relative to value at the top of the vegetation cover is shown parametrically as a function of relative windspeed within the cover layer [Eq. (49)].

base of the live crown (Bergen, 1971; Oliver, 1971, 1975; Jarvis *et al.*, 1976; Albin and Baughman, 1979) is predicted by the present model, but cannot be reconciled with a model that is exponential in physical height.

4. Model predictions of shear stress

The variation of shear stress τ within the cover layer predicted by the present model is most readily presented in the parametric form implied by (38). The profile of relative Reynolds shear stress is

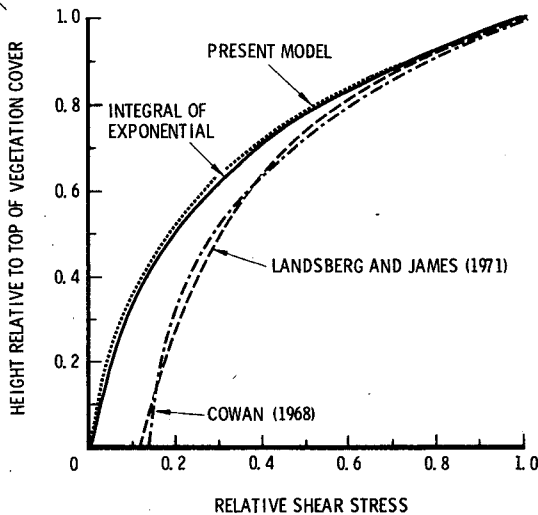


FIG. 8. Profiles of relative Reynolds shear stress versus height for cover with constant drag area density, as predicted by various phenomenological models.

given by

$$\tau(z)/\tau(H) = \frac{-\overline{u'w'}}{(-\overline{u'w'})_H} = (\bar{u}/u_H)^2 G(u_0/\bar{u})/G(u_0/u_H), \quad (49)$$

which is shown graphically in Fig. 7. Each curve shown in Fig. 7 intercepts the abscissa at the value of u_0/u_H , which parameter serves to define the entire profile.

For vegetation cover with uniform drag area density, the present model can readily be compared to other phenomenological models. Using the wind speed versus height profile used for the comparison of Fig. 2, the shear stress versus height prediction of the present model is compared to those for the models of Cowan (1968), and Landsberg and James (1971) in Fig. 8. Also shown in Fig. 8 is the integral of the square of the exponential wind-speed profile, which accounts for most of the variation exhibited by the present model in the uniform layer case, i.e.,

$$\tau(z)/\tau(H) = \left(\int_0^z \bar{u}^2 dz \right) / \left(\int_0^H \bar{u}^2 dz \right) = [(\bar{u}/u_H)^2 - (u_0/u_H)^2] / [1 - (u_0/u_H)^2]. \quad (50)$$

The nonzero shear stress at the surface exhibited by the comparison models is a defect that the present model does not have. So while all the models can reproduce the relative wind-speed profiles found in uniform vegetation layers, the present model seems to do the best job of describing the shear stress distributions measured by Seginer *et al.* (1976) in artificial cover, as shown in Fig. 9.

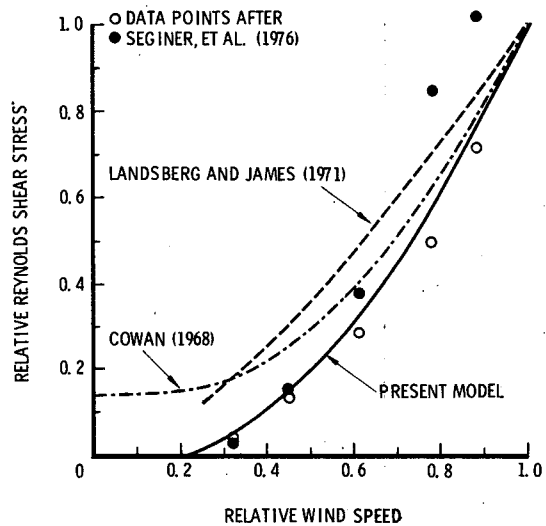


FIG. 9. Comparison of predicted relative shear stress profiles from the models shown in Fig. 8 with data from Seginer *et al.* (1976). Open circles are measurements between elements of the artificial canopy, closed circles are measurements taken directly in the wake of the vertical cylinders comprising the artificial cover layer.

Using the wind speed profiles shown in Fig. 5 and Eq. (49), the relative shear stress profiles for the nonuniform maize canopy studied by Shaw (1977) were constructed and are displayed in Fig. 10. The data points given by Shaw appear to follow the trend of the profile generated by the model, but are displaced downward into the canopy layer ~ 0.1 heights from the model curves.

No other experimental data on turbulent shear stress distributions in nonuniform cover were discovered in a form suitable for direct comparison. The appearance of the profile reported by Hicks and Sheih (1977) for a maize canopy is generally in agreement with the predicted curve of Fig. 10, however, and the profiles inferred by Mayer (1978) for a spruce stand also show the rapid decline in the upper canopy exhibited by this model. Uchijima (1976) reports that a simple exponential in z/H accurately describes measurements of shear stress profiles in wheat and maize, but the data were not presented. Bache and Unsworth (1977) report measured mean wind speed profiles and inferred shear stress profiles in a cotton canopy, both of which fit exponential forms in z/H . They report a uniform foliage density over the upper half of the cover layer, which zone accounted for ~90% of the wind speed reduction and virtually all of the shear stress decay with height.

5. Summary

A highly simplified description of the turbulent flow in a vegetation cover layer was obtained by treating the cover layer as a continuum that affords a body force resisting fluid motion which is equal to the product of the drag area density of the plant parts and the square of the local air speed. The resistive force per unit volume is taken to be opposed to the instantaneous velocity of the fluid and is assumed to be much greater than either viscous forces or fluctuating pressure gradient forces. The resulting expressions are truncated at second order in fluctuating velocity component products, yielding a tractable if oversimplified set of equations for the steady, one-dimensional case. Closure is effected by a phenomenological assumption linking the vertical static pressure field and the mean horizontal wind speed profile.

Profiles of relative wind speed within the vegetation cover stemming from this model appear to be quite robust when compared to available experimental data. For cover layers with a constant drag area density, the wind speed profile degenerates to a simple exponential that mimics previously published phenomenological models.

Profiles of Reynolds shear stress predicted by this model go to zero at the lower boundary, unlike some other phenomenological models. When com-

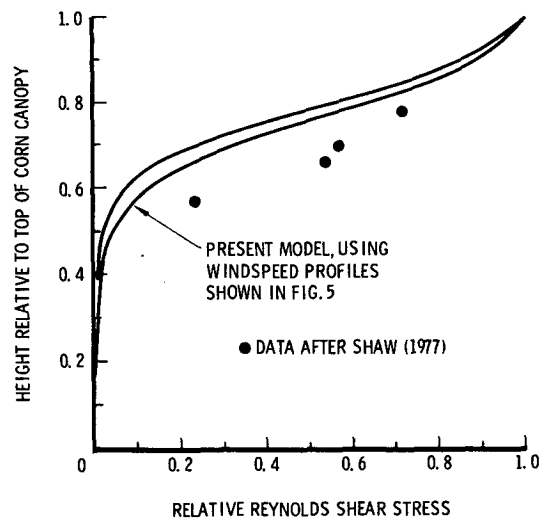


FIG. 10. Comparison of predicted relative shear stress profiles from the present model to data reported by Shaw (1977).

pared to wind tunnel data in an artificial cover layer, the present model performs better than the others. For the scant data on nonuniform cover layers, the present model appears to agree with trends but the shear stress profile appears to be displaced upward in height from the data points.

It should be emphasized that the model presented here is phenomenological in nature, although it rests on forms suggested by a second-order truncation of the equations of turbulent fluid motion with a height-dependent square law body force. The approach invites test and extension.

Acknowledgment. The author wishes to acknowledge the generous assistance of Prof. Roger H. Shaw, University of California at Davis, and Dr. William T. Sommers, USDA Forest Service. Each read an earlier draft of this paper and provided a thoughtful, substantive critique.

APPENDIX

Profiles of $\overline{w'w'}$ and $\overline{u'w'}$

Derivation of (33) and (34) from (27)–(29) and (32) is outlined here. Using boundary conditions (35) and (36) then leads to (38) and (39):

$$\frac{d}{d\zeta} \overline{w'w'} = -\overline{u'w'} - \frac{d\bar{p}}{d\zeta}, \tag{28}$$

$$\overline{w'w'} \frac{d\bar{u}}{d\zeta} = -3\bar{u}\overline{u'w'}, \tag{29}$$

$$\frac{d\bar{p}}{d\zeta} = -\beta\bar{u} \frac{d\bar{u}}{d\zeta}. \tag{32}$$

Using (32) and (29) in (28) gives

$$\frac{d}{d\zeta} \frac{\overline{w'w'}}{\overline{w'w'}} = \frac{\overline{w'w'}}{3\bar{u}} \frac{d\bar{u}}{d\zeta} + \beta\bar{u} \frac{d\bar{u}}{d\zeta}$$

On dividing through by $d\bar{u}/d\zeta$ and rearranging, we have

$$\bar{u}^{1/3} \frac{d}{d\bar{u}} (\overline{w'w'}/\bar{u}^{1/3}) = \beta\bar{u},$$

which can be integrated to give (33)

$$\overline{w'w'} = \bar{u}^{1/3} [(3\beta/5)\bar{u}^{5/3} - c]. \tag{33}$$

Using (32) in (28) and solving for $\overline{u'w'}$ gives

$$\begin{aligned} -\overline{u'w'} &= \frac{d}{d\zeta} \overline{w'w'} - \beta\bar{u} \frac{d\bar{u}}{d\zeta} \\ &= \frac{6\beta}{5} \bar{u} \frac{d\bar{u}}{d\zeta} - \frac{c}{3} \bar{u}^{-2/3} \frac{d\bar{u}}{d\zeta} - \beta\bar{u} \frac{d\bar{u}}{d\zeta} \\ &= \left(\frac{\beta}{5} \bar{u} - \frac{c}{3\bar{u}^{2/3}} \right) \frac{d\bar{u}}{d\zeta}. \end{aligned}$$

Rearranging (27) to the form

$$\bar{u}^{1/2} \frac{d}{d\zeta} (\overline{u'w'}/\bar{u}^{1/2}) = -\bar{u}^2 \tag{27}$$

and using the last expression to replace $d\bar{u}/d\zeta$ gives

$$\begin{aligned} \frac{d}{d\zeta} \left(\frac{-\overline{u'w'}}{\bar{u}^{1/2}} \right) &= \bar{u}^{3/2} = \frac{d\bar{u}}{d\zeta} \frac{d}{d\bar{u}} \left(\frac{-\overline{u'w'}}{\bar{u}^{1/2}} \right) \\ &= (-\overline{u'w'}) / (\beta\bar{u}/5 - c/3\bar{u}^{2/3}) \frac{d}{d\bar{u}} \left(-\frac{\overline{u'w'}}{\bar{u}^{1/2}} \right). \end{aligned}$$

From this form we have

$$\begin{aligned} \left(\frac{-\overline{u'w'}}{\bar{u}^{1/2}} \right) \frac{d}{d\bar{u}} \left(-\frac{\overline{u'w'}}{\bar{u}^{1/2}} \right) \\ = \bar{u} \left(\frac{\beta\bar{u}}{5} - \frac{c}{3\bar{u}^{2/3}} \right) = \beta\bar{u}^2/5 - c\bar{u}^{1/3}/3 \end{aligned}$$

which integrates to

$$\frac{1}{2} \frac{(-\overline{u'w'})^2}{\bar{u}} = \frac{\beta}{15} \bar{u}^3 - \frac{c}{4} \bar{u}^{4/3} + \text{constant}$$

or

$$-\overline{u'w'} = (\beta\bar{u} + 2\beta\bar{u}^4/15 - c\bar{u}^{7/3}/2)^{1/2}. \tag{34}$$

Setting $\overline{w'w'}$ to zero at the lower boundary gives

$$c = (3\beta/5)u_0^{5/3}.$$

Setting $\overline{u'w'}$ to zero at the lower boundary gives

$$\begin{aligned} \beta u_0 &= c u_0^{7/3}/2 - 2\beta u_0^4/15 \\ &= (3/10 - 2/15)\beta u_0^4 = \beta u_0^4/6 \end{aligned}$$

so that

$$\begin{aligned} -\overline{u'w'} &= [(\beta u_0^{3/6})\bar{u} + 2\beta\bar{u}^4/15 - (3\beta/10)u_0^{5/3}\bar{u}^{7/3}]^{1/2} \\ &= \bar{u}^2(2\beta/15)^{1/2}(1 - (9/4)(u_0/\bar{u})^{5/3} \\ &\quad + (5/4)(u_0/\bar{u})^3)^{1/2} \\ &= (2\beta/15)^{1/2}\bar{u}^2 G(u_0/\bar{u}). \end{aligned}$$

Applying the upper surface boundary condition (36) on $-\overline{u'w'}$ gives

$$(-\overline{u'w'})_H = 1/2 C_f u_H^2 = (2\beta/15)^{1/2} u_H^2 G(u_0/u_H)$$

which leads immediately to (38). By identification

$$\beta = 15 C_f^2 / 8 G^2(u_0/u_H), \tag{45}$$

so the expression for $\overline{w'w'}$ can be written as

$$\begin{aligned} \overline{w'w'}/\bar{u}^2 &= (3\beta/5) - c/\bar{u}^{5/3} = (3\beta/5)[1 - (u_0/\bar{u})^{5/3}] \\ &= [9 C_f^2 / 8 G^2(u_0/u_H)][1 - (u_0/\bar{u})^{5/3}] \end{aligned}$$

which is the square of (39).

REFERENCES

Albini, F. A., and R. G. Baughman, 1979: Estimating windspeeds for predicting wildland fire behavior. USDA Agric. Forest Serv. Res. Pap. INT-221, Intermountain Forest and Range Exp. Stn., Ogden, UT, 12 pp.

Allen, L. H., Jr., 1968: Turbulence and wind speed spectra within a Japanese larch plantation. *J. Appl. Meteor.*, **7**, 73-78.

Bache, D. H., and M. H. Unsworth, 1977: Some aerodynamic features of a cotton canopy. *Quart. J. Roy. Meteor. Soc.*, **103**, 121-134.

Baughman, R. G., and F. A. Albini, 1980: Estimating midflame wind speeds. *Proc. Sixth Conf. Fire and Forest Meteor.*, Seattle, WA, Robert E. Martin, Robert L. Edmonds, Donald A. Faulkner, James B. Harrington, Donald M. Fuquay, Brian J. Stocks and Sumner Barr, Eds. Soc. Amer. Foresters, 304 pp. (see pp. 88-92).

Bergen, James D., 1971: Vertical profiles of wind speed in a pine stand. *Forest Sci.*, **17**, 314-321.

—, 1975: An approximate analysis of the momentum balance for the airflow in a pine stand. *Heat and Mass Transfer in the Biosphere*, Part I, D. A. deVries and N. H. Afgan, Eds., Scripta, 495 pp. (see Chap. 18).

Cionco, Ronald M., 1965: A mathematical model for air flow in a vegetative canopy. *J. Appl. Meteor.*, **4**, 517-521.

—, 1972a: A wind-profile index for canopy flow. *Bound.-Layer Meteor.*, **3**, 255-263.

—, 1972b: Intensity of turbulence within canopies with simple and complex roughness elements. *Bound.-Layer Meteor.*, **2**, 453-465.

—, 1978: Analysis of canopy index values for various canopy densities. *Bound.-Layer Meteor.*, **15**, 81-93.

Cowan, I. R., 1968: Mass, heat and momentum exchange between stands of plants and their atmospheric environment. *Quart. J. Roy. Meteor. Soc.*, **94**, 523-544.

Finnigan, J. J., 1979a: Turbulence in waving wheat, I. Mean statistics and Homani. *Bound.-Layer Meteor.*, **16**, 181-211.

—, 1979b: Turbulence in waving wheat, II. Structure of momentum transfer. *Bound.-Layer Meteor.*, **16**, 213-236.

—, and P. J. Mulhearn, 1978a: A simple mathematical model of airflow in waving plant canopies. *Bound.-Layer Meteor.*, **14**, 415-431.

—, and —, 1978b: Modelling waving crops in a wind tunnel. *Bound.-Layer Meteor.*, **14**, 253-277.

- Grace, J., 1977: *Plant Response to Wind*. Academic Press, New York, 204 pp.
- Hicks, B. B., and C. M. Sheih, 1977: Some observations of eddy momentum fluxes within a maize canopy. *Bound.-Layer Meteor.*, **11**, 515-519.
- Holbo, H. R., T. C. Corbett and P. J. Horton, 1980: Aero-mechanical behavior of selected Douglas fir. *Agric. Meteor.*, **21**, 81-91.
- Hsi, G., and J. H. Nath, 1970: Wind drag within simulated forest canopies. *J. Appl. Meteor.*, **9**, 592-602.
- Inoue, E., 1963: On the turbulent structure of airflow within crop canopies. *J. Meteor. Soc. Japan*, **41**, 317-325.
- Jarvis, P. G., G. B. James and J. J. Landsberg, 1976: Coniferous forest. *Vegetation and the Atmosphere*, Vol. 2, *Case Studies*, J. L. Monteith, Ed., Academic Press, 439 pp. (see Chap 7).
- Kondo, Junsei, and Shuhei Akashi, 1976: Numerical studies on the two-dimensional flow in horizontally-homogeneous canopy layers. *Bound.-Layer Meteor.*, **10**, 255-272.
- Landsberg, J. J., and G. B. James, 1971: Wind profiles in plant canopies: studies on an analytical model. *J. Appl. Ecol.*, **8**, 729-741.
- Leuning, R., and P. M. Attiwill, 1978: Mass, heat and momentum exchange between a mature Eucalyptus forest and the atmosphere. *Agric. Meteor.*, **19**, 215-241.
- Maitani, T., 1977a: Vertical transport of turbulent kinetic energy in the surface layer over a paddy field. *Bound.-Layer Meteor.*, **12**, 405-423.
- , 1977b: Some turbulence characteristics in the surface layer over a wheat field. *Ber. Ohara Inst. Landwirtschl. Biol., Okayama Univ.*, **17**, No. 1, 29-46.
- , 1978: On the downward transport of turbulent kinetic energy in the surface layer over plant canopies. *Bound.-Layer Meteor.*, **14**, 571-584.
- , 1979a: A comparison of turbulence statistics in the surface layer over plant canopies with those over several other surfaces. *Bound.-Layer Meteor.*, **17**, 213-222.
- , 1979b: An observational study of wind-induced waving of plants. *Bound.-Layer Meteor.*, **16**, 49-65.
- Mayer, H., 1978: Characteristics of the vertical wind profile within and above a Spruce stand. *Agric. Meteor.*, **19**, 275-293.
- McBean, Gordon A., 1968: An investigation of turbulence within the forest. *J. Appl. Meteor.*, **7**, 410-416.
- Meroney, R. N., 1968: Characteristics of wind and turbulence in and above model forests. *J. Appl. Meteor.*, **7**, 780-788.
- Monteith, J. L., 1975: *Vegetation and the Atmosphere*, Vol. 1, *Principles*. Academic Press, 278 pp.
- Oke, T. R., 1978: *Boundary Layer Climates*. Methuen and Co., 372 pp.
- Oliver, H. R., 1971: Wind profiles in and above a forest canopy. *Quart. J. Roy. Meteor. Soc.*, **97**, 548-553.
- , 1975: Ventilation in a forest. *Agric. Meteor.*, **14**, 347-355.
- Plate, Erich J., 1971: *Aerodynamic Characteristics of Atmospheric Boundary Layers*. U.S. Atomic Energy Commission, 190 pp. [NTIS TID-25465].
- , and A. A. Quraishi, 1965: Modelling of velocity distributions inside and above tall crops. *J. Appl. Meteor.*, **4**, 400-408.
- Rauner, Ju. L., 1976: Deciduous forests. *Vegetation and the Atmosphere*, Vol. 2, *Case Studies*, J. L. Monteith, Ed., Academic Press, 439 pp. (see Chap. 8).
- Reynolds, W. C., and T. Cebeci, 1978: Calculation of turbulent flows. *Topics in Applied Physics*, Vol. 12, *Turbulence*, P. Bradshaw, Ed. (2nd corrected and updated edition) Springer-Verlag, 339 pp. (see Chap. 5).
- Saugier, B., 1976: Sunflower. *Vegetation and the Atmosphere*, Vol. 2, *Case Studies*, J. L. Monteith, Ed., Academic Press, 439 pp. (see Chap. 4).
- Schlichting, Hermann, 1968: *Boundary-Layer Theory*, 6th ed. McGraw-Hill, 747 pp.
- Seginer, I., and P. J. Mulhearn, 1978: A note on vertical coherence of streamwise turbulence inside and above a model plant canopy. *Bound.-Layer Meteor.*, **14**, 512-523.
- , —, E. F. Bradley and J. J. Finnigan, 1976: Turbulent flow in a model plant canopy. *Bound.-Layer Meteor.*, **10**, 423-453.
- Shaw, Roger H., 1977: Secondary wind speed maxima inside plant canopies. *J. Appl. Meteor.*, **16**, 514-521.
- , G. denHartog, K. M. King and G. W. Thurtell, 1974: Measurements of mean wind flow and three-dimensional turbulence intensity within a mature corn canopy. *Agric. Meteor.*, **13**, 419-425.
- Shinn, Joseph Hancock, 1971: Steady state two-dimensional air flow in forests and the disturbance of surface layer flow by a forest wall. Ph.D. thesis, University of Wisconsin, Madison, 91 pp.
- Silversides, R. H., 1974: On scaling parameters for turbulence spectra within plant canopies. *Agric. Meteor.*, **13**, 203-211.
- Thom, A. S., 1971: Momentum absorption by vegetation. *Quart. J. Roy. Meteor. Soc.*, **97**, 414-428.
- Townsend, A. A., 1980: *The Structure of Turbulent Shear Flow*, 2nd ed. Cambridge University Press, 429 pp.
- Uchijima, Z., 1976: Maize and rice. *Vegetation and the Atmosphere*, Vol. 2, *Case Studies*, J. L. Monteith, Ed., Academic Press, 439 pp. (see Chap. 2).
- Wilson, N. Robert, and Roger H. Shaw, 1977: A higher order closure model for canopy flows. *J. Appl. Meteor.*, **16**, 1197-1205.